

# A crustal thickness map of Africa derived from a global gravity field model using Euler deconvolution

Getachew E. Tedla,<sup>1,2</sup> M. van der Meijde,<sup>1</sup> A. A. Nyblade<sup>2,3</sup> and F. D. van der Meer<sup>1</sup>

<sup>1</sup>University of Twente, Faculty of Geo-Information Sciences and Earth Observation (ITC), Enschede, The Netherlands. E-mail: tedla@itc.nl, get11@psu.edu

<sup>2</sup>Department of Geosciences, Pennsylvania State University, University Park, PA 16802, USA

<sup>3</sup>School of Geosciences, The University of the Witwatersrand, Johannesburg, South Africa

Accepted 2011 July 1. Received 2011 June 30; in original form 2011 January 21

## SUMMARY

We develop a new continental scale crustal model for Africa by modelling the free-air gravity anomaly EIGEN-GL04C, which was developed from 30 months of GRACE Level 1B data covering the period from 2003 February to 2005 July, and surface gravity data from seven different sources. From this gravity model, crustal thickness is estimated using 3-D Euler deconvolution, a method that does not rely on *a priori* depth and density constraints. The results are in good agreement (i.e. within 5 km) of seismically determined Moho depth estimates from across the continent, except for narrow tectonic regions, such as rift valleys, and areas where seismic velocity models of the crust indicate a gradational Moho. The results show that crustal thickness is fairly homogeneous, with an average crustal thickness for the whole continent of  $39 \pm 2(SD)$  km. The average Moho depth for most terrains is within 5 km of the continental average, and there is little variability between terrains of different age. The average thickness for Archean, Proterozoic and Palaeozoic crust is 39, 39 and 41 km, respectively. Crustal thickness in sedimentary basins across northern and central Africa varies between 33 and 36 km. Through comparison with global averages for similar-aged terrains, we find that African crustal thickness does not deviate significantly from the thickness of crust in other parts of the world.

**Key words:** Satellite gravity; Gravity anomalies and Earth structure; Dynamics: gravity and tectonics; Crustal structure.

## 1 INTRODUCTION

In this paper, we present a new continental scale crustal model for Africa by modelling gravity data and calibrating the Moho depth estimates against seismically determined estimates. Much of the African continent consists of Archean and Proterozoic crust, some of which has been reworked during younger tectonic episodes. Estimates of crustal structure, and Moho depth in particular, place first-order constraints on tectonic and geochemical processes that have led to crustal formation and evolution. Relatively little is known about the African crust in comparison to other continents, and thus global averages of crustal parameters, including Moho depth, may not reflect the nature of the African crust. Thus, improved estimates of African crustal structure, such as those presented in this paper, are needed.

To develop a new African continental crustal model, we use 3-D Euler deconvolution, a method that does not rely on *a priori* depth and density constraints (Reid *et al.* 1990; Mushayandebvu *et al.* 2001) and therefore can be applied to regions where there are few, if any such constraints. This method is widely used in terrestrial applications to model the source depths of discrete gravity and magnetic anomalies. As explained by Keating (1998) and Silva & Barbosa (2003), the method is particularly good at delineating horizontal and

vertical contacts, making it possible to use this method to estimate the depth of the crust–mantle boundary.

Our results show that crustal thickness across Africa, regardless of the age of the terrain, is similar, deviating by no more than  $\sim 5$  km from a continental average of 39 km. Through comparison of our results with global averages for similar-aged terrains, we also show that African crustal thickness is comparable to crust in other parts of the world.

## 2 DATA

Crustal thickness is computed from the free-air gravity anomaly EIGEN-GL04C, which was developed from 30 months of GRACE Level 1B data covering the period from 2003 February to 2005 July, and surface gravity data from seven different sources (Christoph *et al.* 2008, Fig. 1A). The satellite orbits were used to incorporate lower spherical harmonics up to  $150^\circ$  in to the model, and the remaining higher degrees (i.e.  $150^\circ$ – $360^\circ$ ) were computed from terrestrial gravity data (Christoph *et al.* 2008). The accuracy of the model is generally improved by one order of magnitude from pre-GRACE global models (Reigber *et al.* 2005; Tapley *et al.* 2005; Christoph *et al.* 2008).

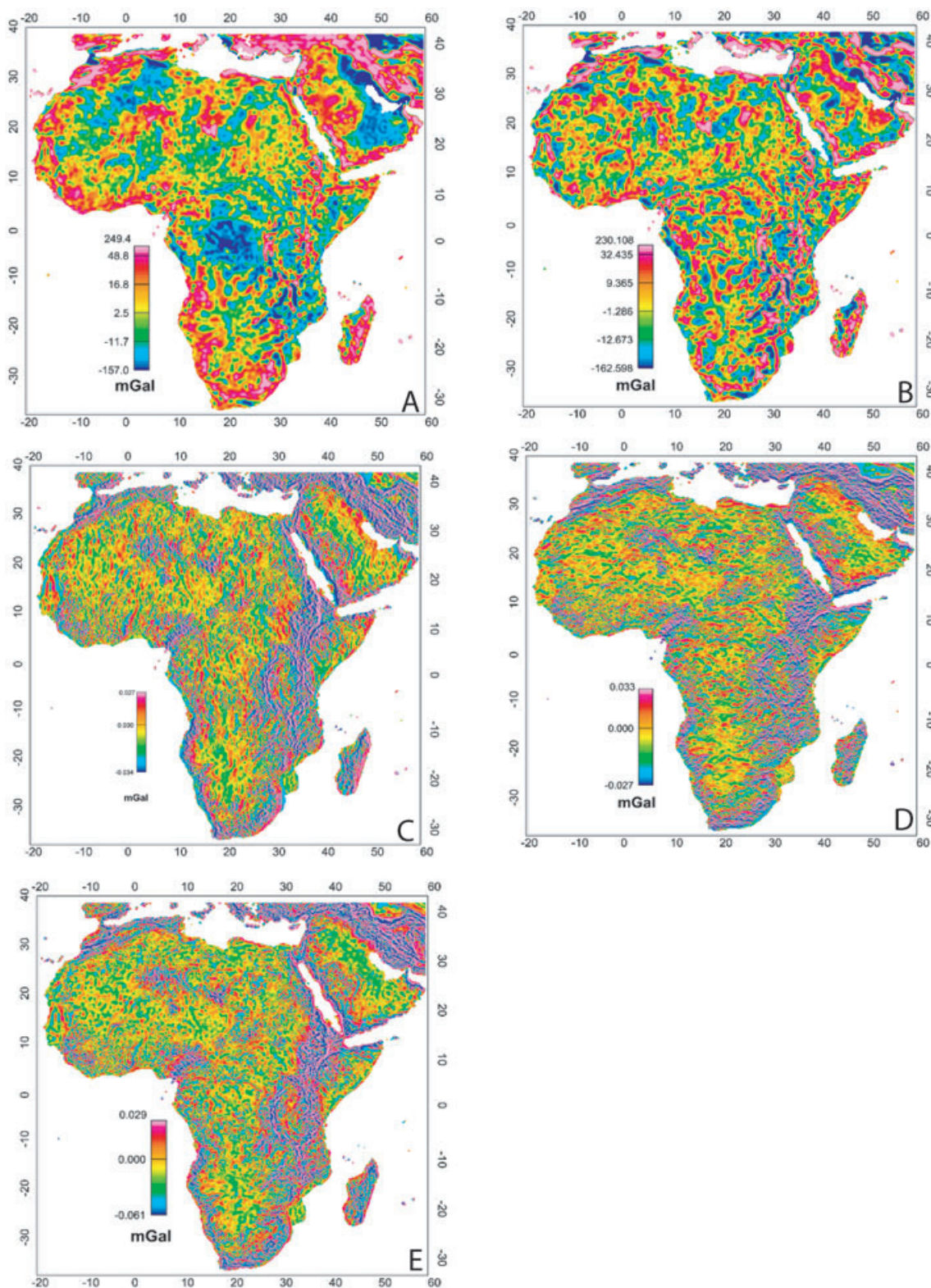


**Figure 1.** Free-air anomaly and input maps to the 3-D Euler equation: (A) EIGEN-GL04C free-air anomaly, (B) High-pass filtered gravity anomaly map (1000 km), (C)  $X$  derivative, (D)  $Y$  derivative and (E)  $Z$  derivative.

### 3 METHODOLOGY

As our main interest is the depth of the crust–mantle boundary, the gravity data are first subjected to a high-pass filter using a 1000-km cut-off wavelength to remove deep mantle sources (Obenson 1974;

Block *et al.* 2009, Fig. 1B). Undesired tapering effects are minimized by expanding the grid up to 20 per cent of the total grid area. We then calculate the  $X$ ,  $Y$ ,  $Z$  derivatives of the filtered gravity anomaly on a  $0.25^\circ$  grid (Figs 1C, D and E) and use them as input to the 3-D Euler equation.

For a detailed explanation of 3-D Euler deconvolution, the reader is referred to Reid *et al.* (1990), Mushayandebvu *et al.* (2004) and Florio *et al.* (2006). A least-squares inversion algorithm is used to solve the Euler equation for an optimum source location. The method involves selecting a structural index value and a square window size, which determines of the number of cells in the gridded data set used in the inversion.

Structural index values can range from 0 to 2, and selecting a structural index is not necessarily straightforward because the index for a single type of interface is not unique. Mushayandebvu *et al.* (2004) discussed the influence of the structural index on location and depth uncertainty using a synthetic anomaly. Their test indicated that the depth to an anomaly could vary significantly with structural index but that the location uncertainties ( $X$  and  $Y$  offset) did not change significantly. Thus, although it may be possible to detect an anomaly using two different structural indices, the depth estimate obtained for each index could be quite different. To estimate crustal thickness using this method, we assume that the crust–mantle boundary is a horizontal sheet or sill-type interface and that it can be represented in an infinite 2-D space. According to Mushayandebvu *et al.* (2001), this geometry should be best resolved using a structural index of 0.5. Therefore, we use a structural index of 0.5, and we provide further justification of this choice in Section 5.2.

The other important modelling variable is the window size. The width of the window influences the depth range for which solutions can be obtained. In general, solutions with depths much greater or much smaller than the width of the window may be unreliable,

resulting from either multiple sources or a source that does not fit the assumed model geometry (i.e. sill, dyke or sphere).

Reid *et al.* (1990) investigated the relationship between anomaly depth and window size, and found that reliable solutions could be obtained within a maximum depth of three times the window size or within a minimum depth equivalent to the window size. They also noted that the window size has to be small enough to discriminate anomalies arising from different sources yet big enough to incorporate deep sources and spatially extensive sources. Therefore, solutions that lay too far from the centre of a window may be unreliable.

Given these considerations, we use a window size of 20 km  $\times$  20 km and only include solutions with a  $X$  and  $Y$  offset less than 5 km (i.e. the spatial uncertainty in the position of the Moho depth estimate  $<5$  km). An uncertainty of  $<5$  km for the locations of the Moho depth values is optimal because larger offsets could possibly allow for the smearing of Moho depth estimates across tectonic boundaries. The selection of the window size is also further justified in Section 5.2.

#### 4 MODEL DESCRIPTION

Our map of crustal thickness for Africa is shown in Fig. 2 and point values are provided as supplemental material (Table S1, Supporting Information). Moho depths for most terrains appear to be similar. The average Moho depth for the entire continent is 39 km and the average for most terrains is within 5 km of the continental average. In general, regions that are associated with large sedimentary basins

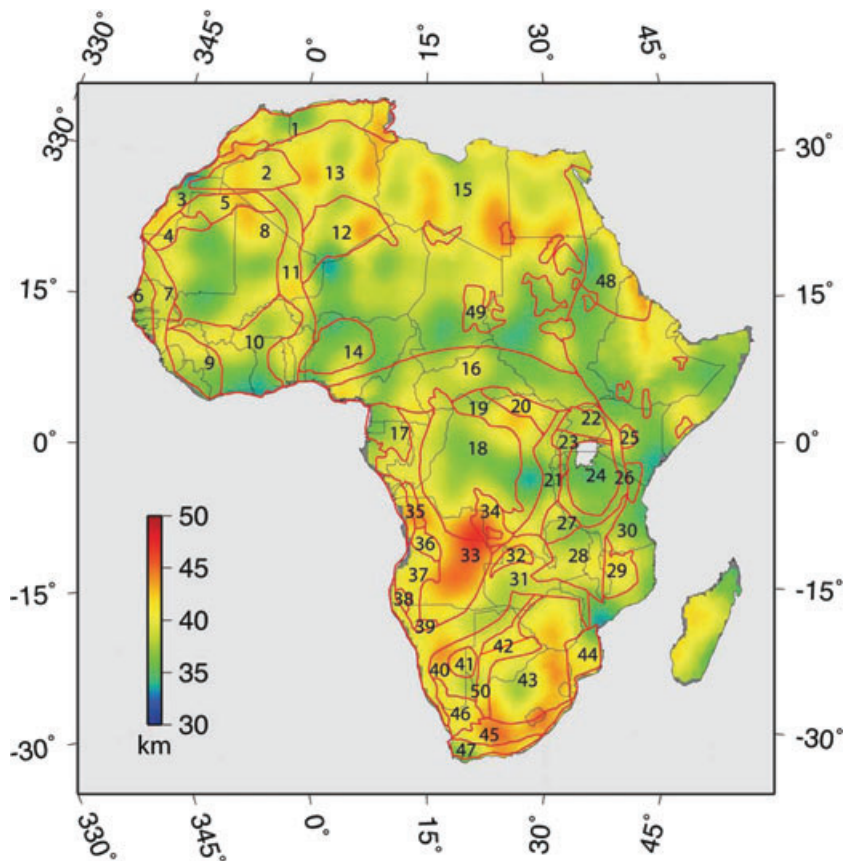


**Figure 2.** Crustal thickness map of Africa. Tectonic regions displayed by red lines are from Begg *et al.* (2009). For explanations of the different terrains and their corresponding codes, see Table 4 and Begg *et al.* (2009).

tend to have thinner crust whereas ancient orogenic belts appear to have somewhat thicker crust. After evaluating the model using seismic estimates of crustal thickness and further examining our selection of the structural index and window size, we discuss our map of crustal thickness in more detail in Section 6.

## 5 MODEL EVALUATION

We use seismic estimates of crustal thickness from receiver function studies and refraction profiles in Africa to evaluate our model. We first examine variations in Moho depth and then compare results for a range of structural indices and window sizes.

### 5.1 Model evaluation using seismic estimates of crustal thickness

Table 1 gives a list of crustal thickness estimates from receiver functions and seismic refraction profiles that we use to evaluate our model. In Fig. 3, we compare our estimates of crustal thickness to the seismic estimates. Our estimates of Moho depth agree to within 5 km of the seismic estimates at 86 per cent of the locations, illustrating that there is reasonably good agreement overall between our Moho depth estimates and those obtained from seismic data. For areas where the Moho depth estimates differ by  $>5$  km, the areas either have a gradational Moho or else are in narrow tectonic regions, such as rift valleys.

For example, a difference of  $>5$  km is observed for several stations in Ethiopia (Table 2, Dugda *et al.* 2005), which are located either in the Afar depression, in the Main Ethiopian Rift or at the boundary between the Ethiopian Plateau and East African rift system (Table 2 and Fig. 3). Similarly, a difference  $>5$  km is found for stations located in the Garoua Rift in West Africa and along the Cameroon volcanic line (Tokam *et al.* 2010). Another example is in South Africa, where our results deviate by more than 5 km from the

seismic estimates where the change in shear wave velocity across the Moho is gradational and not defined by a significant velocity discontinuity (Kgaswane *et al.* 2009, Table 2).

From the above observations, it is apparent that the estimates of crustal thickness obtained for narrow tectonic features or where the crust has a gradational Moho are less reliable. Nevertheless, for most terrains, the Euler derived estimates of crustal thickness are within 5 km of the seismic estimates.

### 5.2 Structural index and window size

We next use a comparison of the seismic estimates of crustal thickness with our model results to evaluate further the choice of the structural index and window size for the Euler deconvolution. To evaluate the influence of window size on crustal thickness estimates, we show the difference between 3-D Euler deconvolution and seismic estimates of crustal thickness for stations in the Tanzania Craton, where crustal structure is fairly simple (Table 3, Dugda *et al.* 2005). We have tested window sizes of 15, 20, 30, 40 and 50 km for a structural index of 0.5. As shown in Table 3, the difference between the Euler deconvolution and seismic estimates of crustal thickness are lowest for a window size of 20 km  $\times$  20 km for all but three stations.

To evaluate the structural index, we fixed the window size to 20 km  $\times$  20 km and then modified the structural index. The difference between Euler deconvolution results and seismic estimates of crustal thickness is below 5 km for 47, 86, 69, 59 and 44 per cent of the stations for indices of 0.0, 0.5, 1, 1.5 and 2, respectively. We have also used scatterplots between our results and seismic estimates of crustal thickness (Fig. 4) to evaluate our choice of structural index. From Fig. 4, it can be seen that the strongest correlation is obtained for a structural index of 0.5. We have also varied both parameters (structural index and window size) simultaneously over the full range of plausible values and do not find better fits

**Table 1.** Sources of seismic estimates of Moho depth used in Fig. 3.

| Source  | Region       | Survey type       |
|---|--------------|-------------------|
| van der Meijde <i>et al.</i> (2003)                   | North Africa | Receiver Function |
| Marone <i>et al.</i> (2003)                           | North Africa | Receiver Function |
| Dugda <i>et al.</i> (2005)                            | Kenya        | Receiver Function |
| Dugda <i>et al.</i> (2005)                            | Tanzania     | Receiver Function |
| Gangopadhyay <i>et al.</i> (2007)                     | West Africa  | Receiver Function |
| Nguuri <i>et al.</i> (2001)                           | South Africa | Receiver Function |
| Dugda <i>et al.</i> (2005)                            | Ethiopia     | Receiver Function |
| Tokam <i>et al.</i> (2010)                            | Cameroon     | Receiver Function |
| Kgaswane <i>et al.</i> (2009)                         | South Africa | Receiver Function |
| Julia <i>et al.</i> (2005)                            | Tanzania     | Receiver Function |
| Dugda <i>et al.</i> (2009)                            | Kenya        | Receiver Function |
| Kosarian (2006)                                       | North Africa | Receiver Function |
| Keranan <i>et al.</i> (2009)                          | Ethiopia     | Refraction        |
| Mohamed <i>et al.</i> (2001)                          | Sudan        | Refraction        |
| Stuart & Zengeni (1987)                               | Zimbabwe     | Refraction        |
| Keller <i>et al.</i> (1994)                           | Kenya        | Refraction        |
| Mechie <i>et al.</i> (1994)                           | Kenya        | Refraction        |
| Wright <i>et al.</i> (2003)                           | South Africa | Refraction        |
| Kwadiba <i>et al.</i> (2003)                          | South Africa | Refraction        |
| Green & Durrheim (1990)                               | South Africa | Refraction        |
| Buness <i>et al.</i> (1992); Mickus & Jallouli (1999) | North Africa | Refraction        |
| Doser <i>et al.</i> (1997)                            | North Africa | Refraction        |
| Seber (1995)  | North Africa | Refraction        |
| Maguire <i>et al.</i> (1994)                          | Kenya        | Refraction        |
| Braille <i>et al.</i> (1994)                          | Kenya        | Refraction        |

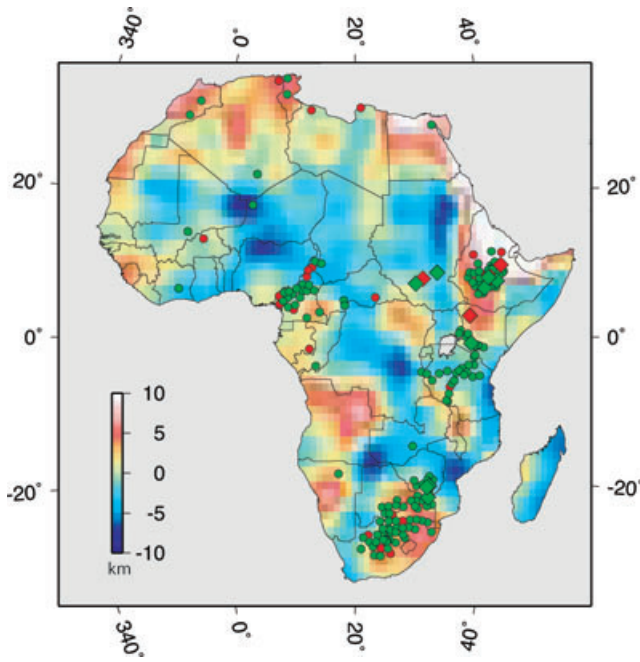


**Figure 3.** Map showing a comparison of crustal thickness estimates. Diamonds show locations of Moho depth estimates from seismic refraction profiles and circles from receiver functions. For green symbols, Moho depth estimates from this study are within 5 km of the seismic estimates and for red symbols they exceed 5 km. The background colour of the map shows the difference between our Moho depth estimates and those from the CRUST2.0 model (Bassin *et al.* 2000).

between the seismic- and gravity-based estimates of Moho depth than shown in Fig. 4 for a structural index of 0.5. Consequently, we conclude that a 20 km  $\times$  20 km window size and a structural index of 0.5 are the optimum parameters for performing the 3-D Euler deconvolution.

## 6 RESULTS

In this section, we examine crustal thickness across the continent with respect to major tectonic terrains, as defined by Begg *et al.* (2009), and compare our results with crustal thickness estimates for similar terrains globally (Durrheim & Mooney 1994; Christensen & Mooney 1995; Rudnick & Fountain 1995). As much of the African continent consists of Precambrian crust, in this comparison we focus mainly on Archean cratons and Proterozoic mobile belts.

The average crustal thickness for all Precambrian terrains is 39 km. To compare crustal thickness between different tectonic provinces, we compute an average value of crustal thickness for each terrain using Moho depth estimates for individual grid elements that are at least 5 km from a terrain boundary. The terrain boundaries are shown in Fig. 2 and the average crustal thickness values are given in Table 4. Because our Moho depth estimates are not well determined for small terrains, we do not report values for the small terrains shown in the Begg *et al.* (2009) terrain map.

### 6.1 Archean terrains

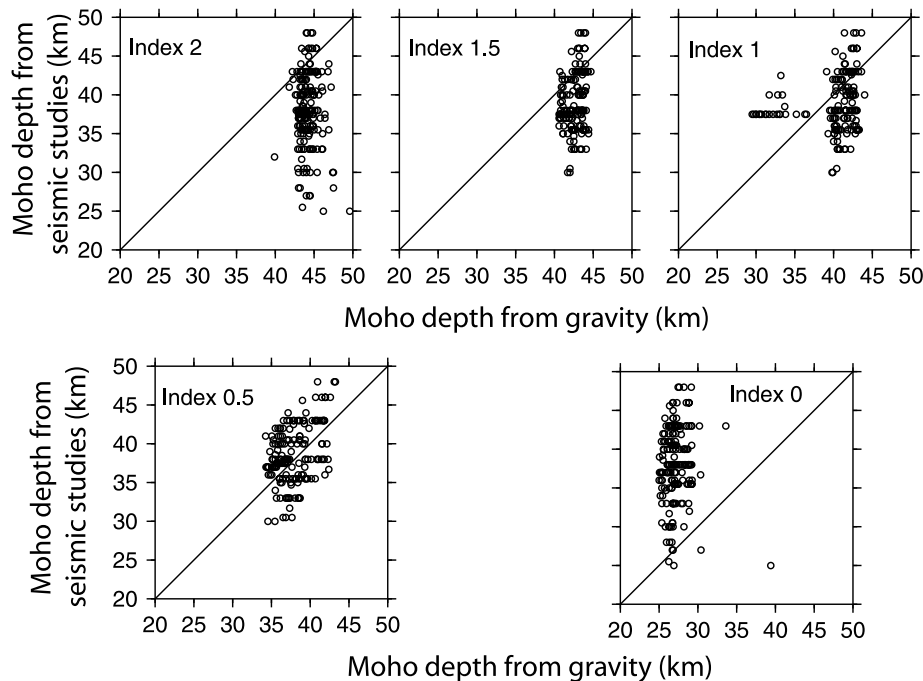
The average crustal thickness of Archean terrains is 39 km (Table 4). Crust in the Reguibat and Man–Leo shields of the West Africa Craton is 42 and 38 km thick, respectively (Table 4 and Fig. 2). For the Congo Craton, the average crustal thickness of the three main Archean blocks, the Gabon–Kamerun, Bomu–Kibalian and the Kasai shields is 38, 39 and 41 km, respectively. In east Africa, the average crustal thickness of the Ugandan (i.e. Basement Complex of northern Uganda) and Tanzania cratons, is 37 and 36 km, respectively (Table 4 and Fig. 2). In southern Africa, the Kaapvaal and Zimbabwe cratons have crust that is 40 km thick on average. These results are in general agreement with global estimates from Christensen & Mooney (1995) and Rudnick & Fountain (1995), who found an average crustal thickness of 38 and 43 km, respectively, for Archean terrains. On the other hand, our range of average crustal thickness values, 36–42 km, is narrower and slightly higher

**Table 2.** Locations where crustal thickness estimates differ by  $>5$  km from seismic estimates.

| Station | Country      | Lon (°) | Lat (°) | Moho depth (km) (This study) | Moho depth (km) (seismic) | Tectonic setting   |
|---------|--------------|---------|---------|------------------------------|---------------------------|--------------------|
| CM29    | Cameroon     | 13.39   | 9.35    | 37                           | 26                        | Garoua Rift        |
| CM30    | Cameroon     | 13.96   | 9.76    | 37                           | 28                        | Garoua Rift        |
| CM31    | Cameroon     | 15.26   | 10.33   | 38                           | 31                        | Garoua Rift        |
| CM18    | Cameroon     | 9.36    | 5.72    | 38                           | 31                        | Gradational Moho   |
| CM13    | Cameroon     | 9.46    | 4.59    | 37                           | 28                        | Gradational Moho   |
| SA40    | South Africa | 27.15   | −25.9   | 37                           | 46                        | Gradational Moho   |
| LBTB    | South Africa | 25.6    | −25.02  | 37                           | 46                        | Gradational Moho   |
| SA22    | South Africa | 22.01   | −27.97  | 41                           | 48                        | Gradational Moho   |
| HVD     | South Africa | 25.5    | −30.61  | 41                           | 48                        | Narrow boundary    |
| SA14    | South Africa | 24.02   | −29.87  | 42                           | 33                        | Narrow boundary    |
| BAHI    | Ethiopia     | 36.76   | 11.47   | 36                           | 44                        | Narrow boundary    |
| FURI    | Ethiopia     | 38.41   | 8.82    | 37                           | 44                        | Rift boundary      |
| SELA    | Ethiopia     | 38.87   | 7.88    | 37                           | 27                        | Rift boundary      |
| CHEA    | Ethiopia     | 38.76   | 8.31    | 37                           | 45                        | Rift boundary      |
| WANE    | Ethiopia     | 40.41   | 10.09   | 40                           | 30                        | Afar depression    |
| TEND    | Ethiopia     | 40.76   | 11.75   | 40                           | 25                        | Afar depression    |
| GEWE    | Ethiopia     | 40.57   | 10.01   | 40                           | 30                        | Afar depression    |
| NAZA    | Ethiopia     | 39.06   | 8.31    | 37                           | 30                        | Main Ethio Rift    |
| GOMA    | Tanzania     | 29.24   | −4.84   | 36                           | 44                        | East Africa Rift   |
| GHAR    | North Africa | 13.09   | 32.12   | 40                           | 30                        | Continental Margin |
| PAB     | North Africa | −4.35   | 39.55   | 42                           | 32                        | Continental Margin |
| ABSA    | North Africa | 7.47    | 36.28   | 39                           | 27                        | Continental Margin |
| KOUM    | North Africa | 26.84   | 37.7    | 39                           | 25                        | Continental Margin |

**Table 3.** Differences (in kilometres) between seismic and gravity estimates of Moho depth in Tanzania for selected window sizes.

| Station | Lon<br>(°) | Lat<br>(°) | Window size (in km) |         |         |         |         |
|---------|------------|------------|---------------------|---------|---------|---------|---------|
|         |            |            | 15 × 15             | 20 × 20 | 30 × 30 | 40 × 40 | 50 × 50 |
| PAND    | 33.03      | -8.95      | 10                  | 6       | 9       | 8       | 7       |
| KIBA    | 36.46      | -5.49      | 11                  | 4       | 10      | 9       | 8       |
| KIBE    | 37.42      | -5.33      | 10                  | 3       | 9       | 9       | 8       |
| KOMO    | 36.6       | -3.82      | 12                  | 3       | 11      | 11      | 10      |
| MTAN    | 33.14      | -7.84      | 9                   | 3       | 8       | 7       | 6       |
| KOND    | 35.64      | -4.87      | 10                  | 2       | 8       | 8       | 7       |
| LONG    | 36.6       | -2.69      | 11                  | 2       | 10      | 9       | 8       |
| SING    | 34.52      | -4.62      | 9                   | 2       | 6       | 6       | 5       |
| TARA    | 35.84      | -3.87      | 11                  | 2       | 9       | 9       | 8       |
| MITU    | 33.85      | -6.01      | 7                   | 2       | 5       | 4       | 2       |
| MBWE    | 34.14      | -4.94      | 8                   | 1       | 6       | 5       | 4       |
| PUGE    | 32.89      | -4.7       | 7                   | 1       | 4       | 3       | 2       |
| URAM    | 31.73      | -5.07      | 7                   | 1       | 5       | 5       | 4       |
| MTOR    | 35.25      | -5.22      | 8                   | 1       | 7       | 6       | 5       |
| BASO    | 34.92      | -4.31      | 5                   | 2       | 4       | 3       | 2       |
| DUNG    | 33.25      | -6.94      | 4                   | 3       | 2       | 1       | 0       |
| INZA    | 29.99      | -5.1       | 4                   | 4       | 2       | 2       | 1       |
| GOMA    | 29.24      | -4.84      | 2                   | 6       | 0       | 0       | 1       |

**Figure 4.** Crustal thickness from this study versus seismic estimates of crustal thickness for structural indices of 0, 0.5, 1, 1.5 and 2. Moho depth estimates are shown only for seismic stations that are either away from tectonic boundaries, not within narrow tectonic features (i.e. rifts), or not in areas with a gradational Moho (see Table 2).

than the range of 29–40 km reported by Durrheim & Mooney (1994) for Archean terrains.

## 6.2 Archean crust with Proterozoic reworking

Similar to the major Archean cratons, the average crustal thickness of Archean terrains with crust that has been reworked during the Proterozoic is 39 km. For the West Africa Craton, we observe that for the northern (region 5) and southern (region 10) parts of the Proterozoic Taoudeni Basin, the crust is, on average, 41 and 38 km thick, respectively. The Man Shield shows a gradient from thicker

crust (42 km) in the northern part toward the Taoudeni Basin and thinner crust (33 km) in its southern region (Fig. 2). The average crustal thickness of the Tuareg and Benin blocks, located in the west African mobile zone, is 39 and 38 km, respectively. The Archean crust that has been reworked during the pan-African orogeny in the eastern Sahara (region 49) is 37 km thick.

## 6.3 Proterozoic crust

The average crustal thickness of Proterozoic terrains is also 39 km. Slightly thicker crust than average is found in the

**Table 4.** Average crustal thickness for tectonic regions defined by Begg *et al.* (2009).

| Age                                      | Map code       | Tectonic region               | Crustal thickness (km) | STDV (km) |
|--|----------------|-------------------------------|------------------------|-----------|
| Archean                                  | 4              | Reguibat Shield               | 42                     | 0         |
|  | 9              | Man–Leo Shield                | 38                     | 1         |
|  | 17             | Gabon–Cameroon Shield         | 38                     | 1         |
|  | 20             | Bomu–Kibalian Shield          | 39                     | 1         |
|  | 22             | Ugandan Craton                | 37                     | 1         |
|  | 34             | Kasai Shield                  | 41                     | 2         |
|  | 24             | Tanzania Craton               | 36                     | 1         |
|  | 43             | Kaapvaal Craton               | 40                     | 3         |
|  |                | <i>Average</i>                | 39                     | 1         |
| Archean crust with Proterozoic reworking | 5              | North of Taoudeni             | 40                     | 1         |
|  | 10             | Man south Taoudeni            | 38                     | 1         |
|  | 37             | Angolan Shield                | 41                     | 1         |
|  | 12             | Tuareg block                  | 39                     | 2         |
|  | 14             | Benin Nigerian block          | 38                     | 2         |
|  | <i>Average</i> | 39                            | 1                      |           |
| Proterozoic                              | 21             | Kibaran                       | 37                     | 1         |
|  | 27             | Bangweleu block               | 37                     | 1         |
|  | 28             | Southern Irumide              | 39                     | 2         |
|  | 42             | Magondi                       | 38                     | 2         |
|  | 50             | Kheis                         | 41                     | 1         |
|  | 45             | Namaqua–Natal                 | 43                     | 1         |
|  | 16             | Obanguides                    | 38                     | 2         |
|  | 30             | Mozambique Orogenic belt      | 38                     | 2         |
|  | 18             | Congo                         | 39                     | 3         |
|  | 11             | Pharusian                     | 39                     | 2         |
|  | 7              | Mauritanides                  | 38                     | 2         |
|  | 2              | Tindouf                       | 40                     | 2         |
|  | 8              | Taudeni                       | 38                     | 2         |
|  | 48             | Nubian Shield                 | 42                     | 1         |
|  | 31             | Damara                        | 39                     | 1         |
|  | 40             | Rehoboth                      | 40                     | 2         |
|  | 26             | Usagaran Ubendian             | 37                     | 1         |
|  | 23             | Ruwenzori                     | 39                     | 2         |
|  | 47             | Saldania                      | 39                     | 2         |
| 49                                       | East Sahara    | 37                            | 2                      |           |
|  | <i>Average</i> | 39                            | 2                      |           |
| Palaeozoic                               | 1              | Atlas                         | 41                     | 2         |
| Phanerozoic cover over Precambrian crust | 19             | Congo Phanerozoic cover       | 41                     | 3         |
|  | 15             | East Sahara Phanerozoic cover | 39                     | 2         |
|  | 6              | Mauritania Phanerozoic cover  | 38                     | 2         |
|  | 44             | Mozambique Phanerozoic cover  | 38                     | 3         |
|  | <i>Average</i> | 39                            | 2                      |           |

orogenic Namaqua–Natal Belt and Nubian Shield (42 and 43 km, respectively). The average for the majority of the terrains is within the standard deviation for the average for all Proterozoic terrains ( $\pm 2$  km). The crustal thickness, for example, in the Proterozoic fold belts in central, eastern and southern Africa is 37–38 km. However, the Taoudeni Basin, with an average crustal thickness of 38 km, has a crustal thickness beneath its interior that is about 3 km thinner. These estimates of crustal thickness are similar to the global averages for Proterozoic terrains of 44 km reported by Rudnick & Fountain (1995) and 42–45 km by Christensen & Mooney (1995).

#### 6.4 Palaeozoic crust

The average crustal thickness of the Palaeozoic Atlas fold belt is 41 km (region 4). In the central part of the belt where

there are sedimentary basins (Schluter 2008), crustal thickness is 5 km thinner than the average value. For Palaeozoic orogens, Rudnick & Fountain (1995) reported a global average thickness of 37 km, similar to the average value for the Atlas fold belt.

#### 6.5 Phanerozoic cover over Precambrian crust

The average crustal thickness of Precambrian terrains that are under Phanerozoic cover is 39 km. This is consistent with a global average of 38 km reported by Christensen & Mooney (1995). Crustal thickness beneath the east Sahara, Congo, Mauritania and Mozambique Phanerozoic cover is 39, 41 and 38 km, respectively (Table 4 and Fig. 2). The East Sahara cover is very extensive and covers several interior basins (Schluter 2008). In these basins, crust is slightly thinner than in other parts of the terrain.

## 7 DISCUSSION

Crustal thickness in Africa is fairly homogeneous with an average crustal thickness for the whole continent of  $39 \pm 2(SD)$  km. Most of the areas do not deviate more than 5 km from the continental average. Furthermore, there is little variability between terrains of different age. The average crustal thickness for Archean, Archean crust reworked in the Proterozoic, Proterozoic, Palaeozoic and Precambrian basement covered with Phanerozoic cover is 39, 39, 39, 41, and 39 km, respectively (Table 4). However, although the crust on average is fairly homogeneous, there are specific areas that show deviations from the average crustal thickness.

Crustal thickness in the composite and complex basins in western and central Africa (Niger, Mali, Guinea, Chad and Sudan) (Schluter 2008), varies between 33 and 36 km. In addition, the crust in the Taoudeni and Congo basins is 3 km thinner than the surrounding Proterozoic and Archean crust.

We also find significant thickening of the crust in the southern part of the Congo Craton in eastern Angola (Fig. 2). Values are up to 10 km thicker than in similar terrains elsewhere in Africa. The origin of this crustal thickening is uncertain. One possible reason for the crustal thickening could be a suture zone between the Congo and the Kalahari Craton along the Damara belt. Alternatively, this could be a region where the Moho is gradational and therefore our estimates of crustal thickness are not reliable.

Overall, our estimates of crustal thickness are in reasonable agreement with estimates from the global crustal model CRUST2.0 (Bassin *et al.* 2000). In many regions, the difference in Moho depth estimates is less than 5 km (see Fig. 3). For instance, the difference is, in general, <2 km in the Tanzania Craton, most of the West African Craton, Limpopo belt, parts of the Kaapvaal Craton, the mobile belts in Zambia and the Kheis belt (Fig. 3). However, there are differences of >5 km in some regions (Fig. 3). Our model is thinner in parts of Mali, Niger, Nigeria, eastern Sudan, the central part of the Congo Basin, southwestern Zambia and central Mozambique (Fig. 3). In contrast, the Euler-based estimates of Moho depth are thicker than CRUST2.0 by >5 km in parts of northern Algeria, Morocco, Tunisia and Egypt.

A comparison with the crustal model from Pasyanos & Nyblade (2007) shows differences in some places that are larger than the differences with CRUST2.0. However, as the resolution of Moho depth estimates in the Pasyanos & Nyblade (2007) model is uncertain, especially along the edges of the continent, a detailed comparison is not warranted.

## 8 CONCLUSION

We have developed a crustal model for Africa that provides new estimates of Moho depth for regions where there are few, if any, published estimates. The reliability of the model has been evaluated through comparison with available crustal thickness estimates from receiver function analysis and seismic refraction profiles. The comparison showed that in areas away from terrain boundaries or narrow terrains, and in areas where the Moho is not gradational, our Moho depth estimates are within 5 km of seismically determined estimates.

The average crustal thickness of the whole continent is 39 km and is fairly uniform (Table 4 and Fig. 2). Somewhat thinner crust is observed beneath sedimentary basins, for example beneath the Taoudeni and Congo basins. The average crustal thickness of terrains of all age in Africa is similar to global averages for terrains of the same age. A comparison of our model with the CRUST2.0

model shows good agreement (i.e. within 5 km) in Moho depth estimates over much of the continent.

## ACKNOWLEDGMENTS

We would like to thank E. Kgaswane and A. Tokam for providing us with receiver function estimates of crustal thickness for southern Africa and Cameroon, respectively, and two anonymous reviewers for helpful comments. This work is supported by the University of Twente, Faculty of Geo-Information Science and Earth Observation and by the National Science Foundation (grant number OISE-0530062). Processing of 3-D Euler deconvolution was performed using Geosoft Oasis-Montaj geophysical software. The GMT software (Wessel & Smith 1998) was partially used to plot figures.

## REFERENCES

- Bassin, C., Laske, G. & Masters, G., 2000. The current limits of resolution for surface wave tomography in North America, *EOS, Trans. Am. geophys. Un.*, **81**, F897.
- Begg, G.C. *et al.*, 2009. The lithospheric architecture of Africa: seismic tomography, mantle petrology, and tectonic evolution, *Geosphere*, **5**, 23–50.
- Block, A.E., Bell, R.E. & Studinger, M., 2009. Antarctic crustal thickness from satellite gravity: implications for the Transantarctic and Gamburtsev Subglacial Mountains, *Earth planet. Sci. Lett.*, **288**, 194–203.
- Braile, L.W., Wang, B., Daudt, C.R., Keller, G.R. & Patel, J.P., 1994. Modeling the 2-D seismic velocity structure across the Kenya Rift, *Tectonophysics*, **236**, 217–249.
- Buness, H. *et al.*, 1992. The EGT'85 seismic experiment in Tunisia: a reconnaissance of the deep structures, *Tectonophysics*, **207**, 245–267.
- Christensen, N.I. & Mooney, W.D., 1995. Seismic velocity structure and composition of the continental crust: a global view, *J. geophys. Res.*, **100**, 9761–9788.
- Christoph, F. *et al.*, 2008. The GeoforschungsZentrum Potsdam Groupe de Recherche de Geodesie Spatiale satellite-only and combined gravity field models: EIGEN-GL04S1 and EIGEN-GL04C, *J. Geodyn.*, **82**, 331–346.
- Doser, D., Keller, G., Harder, S., Miller, K. & Dial, P.J., 1997. Development of a lithospheric model and geophysical database for north Africa, *Tech. Rep. PL-TR-97-2136*, Texas University, EL Paso, TX.
- Dugda, M.T., Nyblade, A.A., Julia, J., Langston, C.A., Ammon, C.J. & Simiyu, S., 2005. Crustal structure in Ethiopia and Kenya from receiver function analysis: implications for rift development in eastern Africa, *J. geophys. Res.*, **110**, doi:10.1029/2004JB003065.
- Dugda, M.T., Nyblade, A.A. & Julia, J., 2009. S-wave velocity structure of the crust and upper mantle beneath Kenya in comparison to Tanzania and Ethiopia: implications for the formation of the east African and Ethiopian Plateaus, *South Afr. J. Geol.*, **112**, 241–250.
- Durrheim, R.J. & Mooney, W.D., 1994. Evolution of the Precambrian lithosphere: seismological and geochemical constraints, *J. geophys. Res.*, **99**, 15 359–15 374.
- Florio, G., Fedi, M. & Pasteka, R., 2006. On the application of Euler deconvolution to the analytic signal, *Geophysics*, **71**, 87–93.
- Gangopadhyay, A., Pulliam, J. & Sen, M.K., 2007. Waveform modelling of teleseismic S, Sp, SsPmP, and shear-coupled PL waves for crust- and upper-mantle velocity structure beneath Africa, *Geophys. J. Int.*, **170**, 1210–1226.
- Green, R. & Durrheim, R., 1990. A seismic refraction investigation of Namaqualand metamorphic complex, South Africa, *J. geophys. Res.*, **95**, 19 927–19 932.
- Julia, J., Ammon, C.J. & Nyblade, A.A., 2005. Evidence for mafic lower crust in Tanzania, East Africa, from joint inversion of receiver functions and rayleigh wave dispersion velocities, *Geophys. J. Int.*, **162**, 555–569.
- Keating, P.B., 1998. Weighted Euler deconvolution of gravity data, *Geophysics*, **63**, 1595–1603.

- Keller, G.R., Mechie, J., Braile, L.W., Mooney, W. & Prodehl, C., 1994. Seismic structure of the uppermost mantle beneath the Kenya rift, *Tectonophysics*, **236**, 201–216.
- Keranen, K.M., Klempner, S.L., Julia, J., Lawrence, J.F. & Nyblade, A.A., 2009. Low lower crustal velocity across Ethiopia: is the main Ethiopian Rift a narrow rift in a hot craton? *Geochem. Geophys. Geosyst.*, **10**, 1525–2027.
- Kgaswane, E.M., Nyblade, A.A., Julia, J., Dirks, P.H., Durrheim, R.J. & Pasyanos, M.E., 2009. Shear wave velocity structure of the lower crust in southern Africa: evidence for compositional heterogeneity within Archean and Proterozoic terrains, *J. geophys. Res.*, **114**, doi:10.1029/2008JB006217.
- Kosarian, M., 2006. Lithospheric structure of North Africa and western Eurasia, *PhD thesis*, The Pennsylvania State University.
- Kwadiba, M., Wright, C., Kgaswane, E., Simon, R. & Nguuri, T.K., 2003. Pn arrivals and lateral variations of Moho geometry beneath the Kaapvaal craton, *Lithos*, **71**, 393–411.
- Maguire, P., Swain, C., Masotti, R. & Khan, M., 1994. A crustal and uppermost mantle cross-sectional model of the Kenya Rift derived from seismic and gravity data, *Tectonophysics*, **236**, 217–249.
- Marone, F., van der Meijde, M., van der Lee, S. & Giardini, D., 2003. Joint inversion of local, regional and teleseismic data for crustal thickness in the Eurasia–Africa plate boundary region, *Geophys. J. Int.*, **154**, 499–514.
- Mechie, J., Keller, G.R., Prodehl, C., Gaciri, S., Braile, L., Mooney, W., Gajewski, D. & Sandmeier, K., 1994. Crustal structure beneath the Kenya Rift from axial profile data, *Tectonophysics*, **236**, 179–200.
- Mickus, K. & Jallouli, C., 1999. Crustal structure beneath the Tell and Atlas Mountains (Algeria and Tunisia) through the analysis of gravity data, *Tectonophysics*, **314**, 373–383.
- Mohamed, A.Y., Ashcroft, W.A. & Whiteman, A., 2001. Structure development and crustal stretching in the Muglad basin, southern Sudan, *J. Afr. Earth Sci.*, **32**, 179–191.
- Mushayandevu, M.F., van Driel, P., Reid, A.B. & Fairhead, J.D., 2001. Magnetic source parameters of two-dimensional structures using extended Euler deconvolution, *Geophysics*, **66**, 814–823.
- Mushayandevu, M.F., Lesurz, V., Reid, A.B. & Fairhead, J.D., 2004. Grid Euler deconvolution with constraints for 2D structures, *Geophysics*, **69**, 489–496.
- Nguuri, T.K. *et al.*, 2001. Crustal structure beneath southern Africa and its implications for the formation and evolution of the Kaapvaal and Zimbabwe cratons, *Geophys. Res. Lett.*, **28**, 2501–2504.
- Obenson, G., 1974. A 1973 Gravimetric Geoid of Africa, *Geophys. J. R. astr. Soc.*, **37**, 271–283.
- Pasyanos, M.E. & Nyblade, A.A., 2007. A top to bottom lithospheric study of Africa and Arabia, *Tectonophysics*, **444**, 27–44.
- Reid, A.B., Allsop, J.M., Granser, H., Millet, A.J. & Somerton, I.W., 1990. Magnetic interpretation in three dimensions using Euler deconvolution, *Geophysics*, **55**, 80–91.
- Reigber, C., Schmidt, R., Flechtner, F., König, R., Meyer, U., Neumayer, K.H., Schwintzer, P. & Zhu, S.Y., 2005. An earth gravity field model complete to degree and order 150 from GRACE: EIGEN-GRACE02S, *J. Geod.*, **39**, 1–10.
- Rudnick, R.L. & Fountain, D.M., 1995. Nature and composition of the continental crust: a lower crustal perspective, *Rev. Geophys.*, **33**, 267–309.
- Schluter, T., 2008. *Geological Atlas of Africa: With Notes on Stratigraphy, Tectonics, Economic Geology, Geohazards, Geosites and Geoscientific Education of Each Country*, 2nd edn, Springer-Verlag, Berlin, 307 pp.
- Seber, D., 1995. Lithospheric and Upper Mantle Structure beneath Northern Morocco and Central Syria, *PhD thesis*, Cornell University.
- Silva, J. B.C. & Barbosa, V.C.F., 2003. 3D Euler deconvolution: theoretical basis for automatically selecting good solutions, *Geophysics*, **68**, 1962–1968.
- Stuart, G. & Zengeni, T., 1987. Seismic crustal structure of the Limpopo mobile belt, Zimbabwe, *Tectonophysics*, **144**, 323–335.
- Tapley, B. *et al.*, 2005. GGM02—An improved Earth gravity field model from GRACE, *J. Geod.*, **79**, 467–478.
- Tokam, A.K., Tabod, C.T., Nyblade, A.A., Julia, J., Wiens, D.A. & Pasyanos, M.E., 2010. Structure of the crust beneath Cameroon, West Africa, from the joint inversion of Rayleigh wave group velocities and receiver functions, *Geophys. J. Int.*, **183**, 1061–1076.
- van der Meijde, M., van der Lee, S. & Giardini, D., 2003. Crustal structure beneath broad-band seismic stations in the Mediterranean region, *Geophys. J. Int.*, **152**, 729–739.
- Wessel, P. & Smith, W., 1998. New, improved version of Generic Mapping Tools released, *EOS, Trans. Am. geophys. Un.*, **79**, 579.
- Wright, C., Kgaswane, E.M., Kwadiba, M., Simon, R., Nguuri, T. & McRae-Samuel, R., 2003. South African seismicity, April 1997 to April 1999, and regional variations in the crust and uppermost mantle of the Kaapvaal craton, *Lithos*, **71**, 369–392.

## SUPPORTING INFORMATION

Additional Supporting Information may be found in the online version of this article:

**Table S1.** Point values.

Please note: Wiley-Blackwell are not responsible for the content or functionality of any supporting materials supplied by the authors. Any queries (other than missing material) should be directed to the corresponding author for the article.